

# DISTRIBUTED CONVERTER FOR HIGH-BRIGHTNESS BREMSSTRAHLUNG GENERATION

*E.Z. Biller, V.I. Nikiforov, A.Eh. Tenishev, A.V. Torgovkin, V.L. Uvarov, V.A. Shevchenko,  
I.N. Shlyakhov, B.I. Shramenko, V.F. Zhiglo*  
*National Science Center "Kharkov Institute of Physics and Technology", Kharkov, Ukraine*  
*E-mail: zhiglo@kipt.kharkov.ua*

The novel type of the converter to transform a high-density electron beam into bremsstrahlung has been developed and investigated. To increase the thermal stability of the converter by means of a growth of the heat-exchange effectiveness in the area of the bremsstrahlung generation a braking media has been performed as the shot evenly distributed in the cooling water. The results of the computer simulation, thermophysical analysis and experimental study of the converter version on the basis of Pb shot are represented. The possibility of essential increase of the permissible electron beam density as well as reduction of the induced activity and water discharge in comparison with plate-type converter from tantalum is shown.

PACS: 03.50.-z; 07.05.Tp; 07.85.Fv; 29.20.Ej; 44.05.+e

## 1. INTRODUCTION

The main method of providing high-energy bremsstrahlung (HEB) (or X-ray) sources of high intensity ( $>1\text{ kW/cm}^2$ ) for photonuclear technologies lies in the generation and conversion of an accelerated electron beam having an energy  $\geq 40$  MeV and an energy flux density  $\geq 10\text{ kW/cm}^2$ . Taking into account a high level of absorbed radiation power in the converter, it is vital to keep an adequate heat resistance of the latter. This can be provided by creating an efficient cooling scheme. Besides, the converter gets activated under the action of a mixed  $\gamma, n$ -radiation generated in it. Therefore, in deciding on a particular material of the converter one must also take into account the activation reactions (preferably with production of radionuclides that have the minimum half-life period).

A water-cooled tantalum plate converter is one of the traditional devices for providing powerful HEB sources (e.g., see [1]). Its major drawback is the production of Ta-182 isotope with the half-life period  $T_{1/2}=115$  days in the radiative capture reaction  $^{181}\text{Ta}(n,\gamma)^{182}\text{Ta}$ .

In view of the mentioned things, we propose a radically new type of the converter in the form of a metallic shot, which is cooled with pressurized water (referred to as a distributed converter) [2]. As an example, the paper presents a detailed study on a variant of a lead shot-based converter.

## 2. COMPARATIVE ANALYSIS OF THE DISTRIBUTED Pb CONVERTER AND THE Ta PLATE CONVERTER

Simulation of bremsstrahlung sources that use converters in the form of a set of tantalum plates and also as leaden shot was carried out for the electron linac KUT-30 conditions [3]. The simulation was performed with the program system PENELOPE/2006 as the basis [4].

### 2.1. SIMULATION CONDITIONS

In simulation, the energy spectrum of accelerated electrons and their density distribution in the transverse plane were most closely approximated to those measured in experiments. The computations were made for

the electron energy at the maximum of the spectrum  $E_0=40$  MeV. The geometry of output devices for reproduction of the simulated HEB source also corresponded to real conditions of the KUT-30 accelerator (Fig. 1).

The exit window of the accelerator consists of the input 1 and output 2 titanium foils, 50  $\mu\text{m}$  in thickness. The 4 mm spacing between the foils is filled with cooling water.

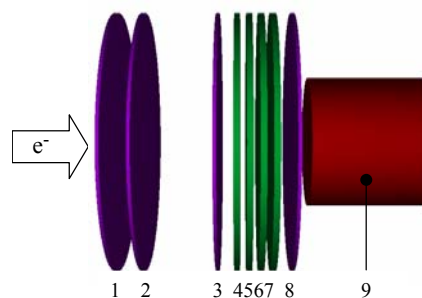


Fig. 1. Configuration of accelerator KUT-30 output devices under conditions of HEB radiation

The converter unit includes the input foil 3, four plates 4, 5, 6, 7 and the output foil 8. The spacings between the foils and plates are filled with water.

The tantalum-based converter consists of four plates, each being 1 mm thick. The plates are separated by water-filled spacings, 1.75, 1.5, 1.5, 2.75 mm in width (in the direction from the input foil to the output foil). So, the distance between the foils is 13 mm.

The lead-based converter consists of four plates, each being 1.82 mm thick. The water spacings in this case measure to be 1.363, 1.0, 1.0, 1.0, 1.363, respectively. The total thickness of the plate assembly makes  $8.26\text{ g/cm}^2$ . This corresponds to the use of the leaden shot with a bulk density of  $6.88\text{ g/cm}^3$  at a shot layer thickness of 1.2 cm.

The test target unit presents a water-cooled cylinder 9, 2 cm in diameter and in height. In the computations, natural zinc was considered as a target material for production of  $^{67}\text{Cu}$  isotope by the reaction  $^{68}\text{Zn}(\gamma, n)^{67}\text{Cu}$ . The target is separated from the converter by foil 8. The distance from the cylinder to the output foil of the converter is 2 mm.

## 2.2. DESCRIPTION OF e,X-RADIATION

As the initially “pure” electron beam of energy  $E_0$  goes deep into the converter, it gets transformed into a flux of mixed e,X-radiation. The composition of the flux along the path of radiation formation depends on the  $E_0$  value, the braking medium and the detection plane position. The e,X-radiation state can be described by the characteristics such as the conversion ratio ( $E_{gr}/E_{beam}$ ) and the secondary emission factor ( $E_{gr}/E_{el}$ ), where  $E_{beam}$  is the total energy of accelerated electrons;  $E_{el}$ ,  $E_{gr}$  are, respectively, the integrated energies of electrons and photons that cross the detection plane on the radiation axis. In this case, it is advisable to measure the distance from the onset of beam slowing down to the plane of detection in the so-called stopping thickness units. Similarly to the well-known mass thickness unit, which is determined as a product of the layer thickness by the layer material density, stopping thickness unit (stu) of any material layer is determined as a ratio of layer thickness to the average total range  $r_0$  of the electron of specified energy in the given material in the continuous slowing-down approximation. In stu terms, the behavior of radiation characteristics for substances in a wide atomic number and energy  $E_0$  range becomes substantially unified [5].

## 2.3. SIMULATION RESULTS

The computational results for the performance of the radiation field generated in the converter of each type are presented in Figs.2 to 5. The range of values, which refer to the converter, is separated by the dashed line and is denoted with the “C” letter.

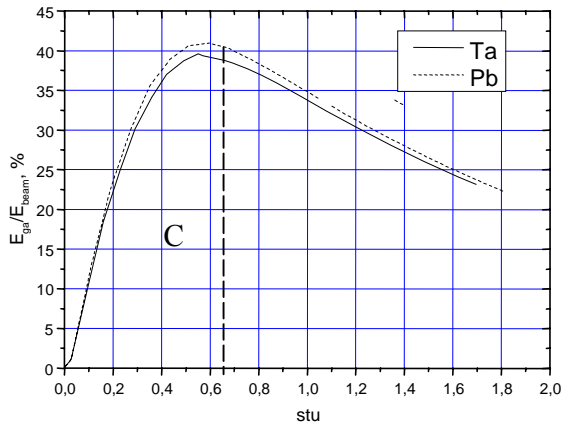


Fig.2. Electron-to-photon energy conversion coefficient

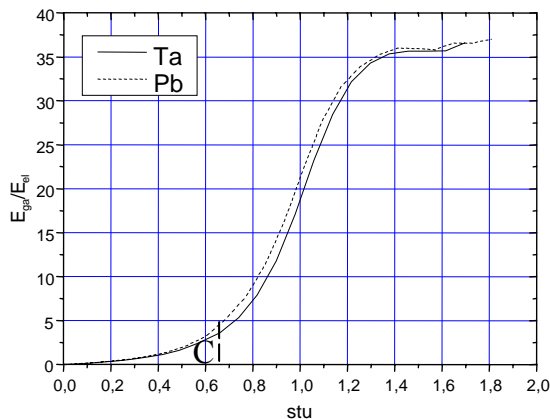


Fig.3. Secondary emission factor

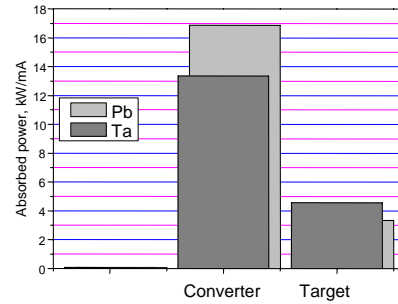


Fig.4. Absorbed power in the converters and the test target

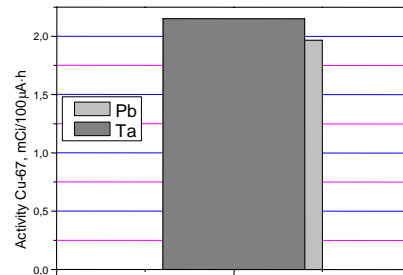


Fig.5. Test Zn-target activity

As it can be seen from the given data, both types of the converters show similar values of radiation characteristics, absorbed radiation power and the rate of isotope generation in the test target.

## 3. THERMOPHYSICAL ANALYSIS OF THE DISTRIBUTED CONVERTER

The optimization in the geometry of the braking medium of the converter has been aimed at improving the efficiency of its cooling by increasing the heat exchange surface. Generally speaking, the converter in the form of a set of plates can also be related to the category of distributed ones. However, in this case, the heat exchange surface can be increased only in two coordinates. The advantage of a three-dimensional uniform distribution of spherical pellets consists not only in an additional surface extend, but also in a substantial enhancement of heat transfer rate. This effect occurs in the fillings and in porous media owing to cooling flow turbulization [6].

### 3.1. HEAT EVOLUTION AND BOUNDARY CONDITIONS

The coordinate system used in the solution of the heat problem is shown in Fig.6.

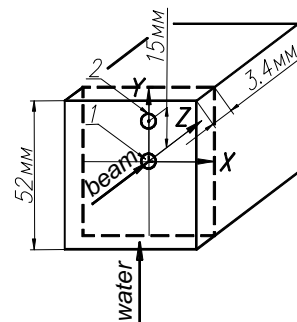


Fig.6. Heat model of the leaden converter.  
1 – peak density of the electron beam;  
2 – effective radius of heating

The thermal power density is satisfactorily approximated by the relationship

$$f(R, Z) = a1 \cdot \exp \left[ - \left( \frac{R}{0.009} \right)^{2.4} - \left( \frac{Z - 0.0034}{0.0044} \right)^2 \right], \quad (1)$$

where  $R^2 = X^2 + Y^2$  is measured in  $m$ . At an average current of  $220 \mu A$  the parameter  $a1$  makes  $2.5 \cdot 10^9 \text{ W/m}^3$ .

Taking into account a high thermal conductivity of filling materials, the thermal conductivity of water can be neglected, considering that the heat exchange between the shots occurs only due to heat transfer of water downstream.

As it follows from (1),  $f(R, Z)$  has its maximum at  $Z=0.0034 \text{ m}$  shown by a dashed line in Fig.6. Neglecting the heat transfer by liquid along the  $Z$ -axis, it can be considered that the maximum temperature distribution also occurs in this plane.

The heat transfer coefficient on the surface of each pellet is derived from  $\alpha = Nu \cdot k / d_e$ , where  $k$  is the water thermal conductivity,  $d_e$  is the hydraulic pore diameter. At the shot diameter  $d$  we have

$$d_e = \frac{2}{3} \cdot d \cdot \frac{\Pi}{1 - \Pi}, \quad (2)$$

where  $\Pi$  is the coefficient of porosity. A close packing of pellets with  $\Pi = 0.26$  was assumed to be most probable. For the Nusselt number  $Nu$ , we have used the expression, which is little dependent on the pellet shape [7]

$$Nu = 4 + K \cdot (A1 \cdot Re_e^2 + A2 \cdot Re_e^3)^{1/4} \cdot Pr^{1/3}, \quad (3)$$

where  $K = 0.17$ ,  $Pr$  is the Prandtl number,  $Re_e$  is the Reynolds number,  $Re_e = V_e \cdot d_e / \nu$ ,  $\nu$  being the kinematic viscosity of water,  $A1 = 133$ ,  $A2 = 2.33$ . The water flow velocity in pores  $V_e$  is calculated from the filtration rate  $V_f$  as  $V_e = V_f / \Pi$ ,  $V_f = N / s$ , where  $N$  is volumetric water discharge,  $s$  is the cross section of the filling. Using the thermophysical parameters of water at a temperature of  $40^\circ C$  we find  $\alpha = 8.63 \cdot 10^4 \text{ W/(m}^2 \cdot K)$  at  $N = 10 \text{ l/min}$ . To attain these heat transfer coefficient values in narrow straight channels, the water flow rate should be approximately 6 times greater (see ref. [1]).

The water temperature in the filling necessary for determining the boundary conditions on the pellet surface was found from the expression

$$t_w(X, Y, Z) = t_0 + \frac{1}{V_f \rho_w C_w} \int_{-0.026}^Y f \left( (X^2 + Y^2)^{1/2}, Z \right) dy, \quad (4)$$

where  $\rho_w$  and  $C_w$  are, respectively, the density and heat capacity of water;  $t_0 = 30^\circ C$  is the converter inlet temperature of water. The water heating by radiation was neglected. The temperature distribution (4) under KUT-30 beam parameters is represented by the lower curve in Fig.7.

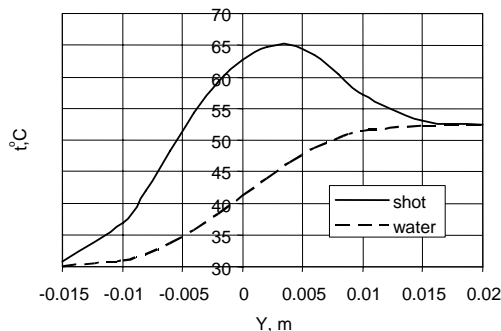


Fig.7. Temperature distribution in the converter

It follows from expression (4) that the water temperature is dependent on  $Y$ . This fact as well as the violation of axial symmetry of the  $f(R, Z)$  function for off-axis pellets calls for a three-dimensional code in solving the heat problem. If the water temperature and the power density are taken to be constant within the pellet volume and equal to their values at the pellet center, then it becomes possible to use two-dimensional programs. The error made in this case can be estimated by making use of the linearity of the heat problem as well as the data of Fig.7 and expression (4).

Thus, the error associated with neglecting the temperature gradient in water will be equal to the water temperature difference at the points corresponding to the center of the pellet and its surface, this being  $\pm 1.3^\circ C$  (see Fig.7). If the power density in the field of one pellet is assumed to be uniform, then the relative error in the temperature distribution would be  $\Delta T/T < (f(Y_s, Z) - f(Y_c, Z)) / f(Y_c, Z)$ , where  $Y_s$ ,  $Y_c$  are the ordinates of the pellet surface and its center, respectively. Using relation (1) it can be demonstrated that  $\Delta T/T < \pm 3.6\%$ . Taking into consideration the insignificance of the given errors for estimative calculations, the two-dimensional approximation was used for solving the heat problem.

### 3.2. THE CONVERTER TEMPERATURE

The time-averaged temperature of the pellet center, depending on their position on the  $Y$ -axis for  $Z=0.0034 \text{ m}$ , is shown in Fig.7. The shift of the temperature peak away from the center of filling is the result of heat transfer by the water flow. The maximum temperature makes  $65.09^\circ C$ .

The spherical symmetry of the calculated temperature distribution inside the pellet (Fig.8) is a consequence of two-dimensionality of the adopted model. The calculation was performed for the pellet located at the point  $Y = 0.004 \text{ m}$ . In this case, the temperature of this pellet center is maximal in the filling (Fig.7).

The pulsed temperature variation was determined by solving numerically the nonstationary heat problem for the electron beam with a pulse length of  $3.5 \mu s$  and a pulse repetition rate of  $150 \text{ Hz}$ . The highest pulsed temperature of the center of the pellet and of its surface was  $80.5^\circ C$  and  $68.8^\circ C$ , respectively.

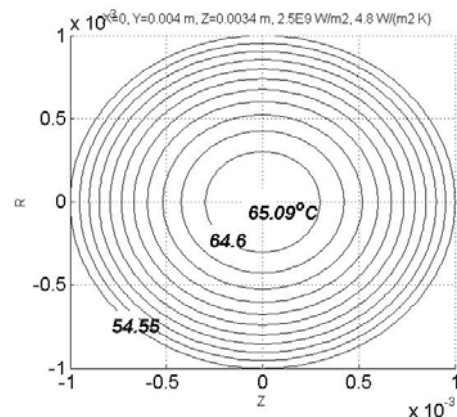


Fig.8. Temperature distribution in the pellet

Using the technique of ref. [7], it can be demonstrated that the calculated  $\alpha$  value is in agreement with the value of water pressure in the converter inlet fitting  $P = 3.76 \cdot 10^5 \text{ Pa}$ .

The pellet surface temperature 68.8°C provides a sufficient reliability of thermal conditions with regard to boiling of water initiated by instabilities in the beam parameters and the water flow. Assuming a stable operation of both the accelerator and the cooling system, as well as a possible overvaluation of Nu from formula (3) by  $\delta=25\%$  [6], it appears possible to estimate a permissible increase in the power of the converted electron beam. If relation (1) is written down as  $f(R,Z) = aI \cdot \varphi(R,Z)$ , and expression (4) is written as  $t_w(R,Z) = aI \cdot D(R,Z)$ , then the maximum average thermal power density  $aI(t_s)$  that corresponds to the pellet surface temperature  $t_s$  can be found from the expression

$$aI(t_s) = (t_s - t_0) \lambda \left[ \frac{dd_e \varphi(R,Z)}{6(1-\delta)kNu} + \frac{D(R,Z)}{V_f \rho_w C_w} \right]^{-1}. \quad (5)$$

Here the parameter  $\lambda=0.63$  takes into account the rise in the surface temperature during the pulse and, as numerical calculations show, depends only slightly on the pellet diameter in the  $0.8 \text{ mm} \leq d \leq 2 \text{ mm}$  range.

The relationship (5) obtained in the approximation of heat generation uniformity in the pellet volume is well confirmed by numerical calculations and shows that:

1. the rise in the pellet temperature up to water boiling  $t_s=100^\circ\text{C}$  permits a 1.6 times increase in the  $aI$  value, i.e., bringing the average beam power up to 12 kW;
2. the reduction in the pellet diameter to  $d=0.82 \text{ mm}$  at  $t_s=100^\circ\text{C}$  enables one to increase the beam power by a factor of 2.2;
3. a 1.6 times increase in the water flow rate at  $d = 2 \text{ mm}$  and  $t_s = 100^\circ\text{C}$  permits a 2.4 times increase in the beam power and in the bremsstrahlung power respectively.

Cases 2 and 3 call for an increase in the water pressure  $P$  up to  $10^6 \text{ Pa}$ . So, if this pressure value is presumed attainable, then the average beam power 18.5 kW can be considered as the maximum power for that converter under the accelerator KUT-30 conditions.

#### 4. EXPERIMENTAL INVESTIGATION OF THE CONVERTER

To perform experimental studies, a prototype distributed-type converter was manufactured. It includes an aluminum casing with a rectangular cavity. The narrow side of the casing has a charge hole to bulk the shot. In its top and bottom parts there are cooling water inlet and outlet pipes. The cavity was filled with lead shots, 2 mm in diameter. The composition of the shot also included antimony and arsenic as attached foreign materials.

The HEB source based on a new-type converter was investigated experimentally at the electron accelerator KUT-30. Directly behind the converter, there were arranged Ni and Sn foils to determine the HEB flux profile by the photonuclear converter technique [8]. The electron energy was measured to be 32 MeV.

First, the converter and the foils were activated for 2 hours at a beam current of 8.6  $\mu\text{A}$ . Figure 9 shows the HEB flux profile reconstructed by scanning the surface activity of the Sn foil with a gamma-scanner. Then the accelerator was switched to the mode of operation with an average current of 260  $\mu\text{A}$ , at which the converter

was irradiated for 10 minutes. This time is sufficient for the shot to reach the heat equilibrium. Thirty minutes after the exposure the shot was extracted from the casing, was examined externally and dosimeter measurements were made over the course of 66 hours.

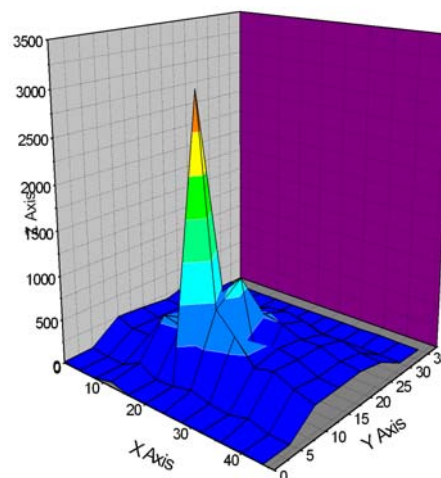


Fig.9. HEB flux density distribution

For this time the contact dose rate decreased from 2 down to 0.4 mSv/h. The external appearance of the shot after irradiation remained practically the same.

The undertaken gamma-spectrometry analysis of individual pellets has revealed that their activity varies within three orders of magnitude depending on the pellet location in relation to the beam. The main contribution to the activity is given by the Pb-203 isotope, which is produced in the  $^{204}\text{Pb}(\gamma,n)^{203}\text{Pb}$  reaction. This is also confirmed by the time of radiation “cooling” of the shot, which has appeared to be close to the half-life period of Pb-203 (51.8 h). The appearance of Sb and As isotopes in the spectrum is due to impurities.

On the 9<sup>th</sup> day after the exposure, the spectrometer studies have shown that the peak heights of both lead and impurities became approximately the same. This encourages us to state that beginning with this period the shot activity level is determined by the impurities, which are absent in pure lead.

#### CONCLUSIONS

Numerical simulation has shown insignificant differences between the characteristics of photon beams produced with the use of a distributed lead shot-based converter and a traditional Ta-plate converter. At the same time, compared to the Ta plate-based converter, the distributed Pb shot-based converter calls for a moderate water discharge, has a low level of induced activity and provides at least a 1.6 times increase in the bremsstrahlung intensity through increasing the permissible electron flux density.

#### REFERENCES

1. V.I. Nikiforov, V.L. Uvarov, V.Ph. Zhyglo. Thermophysical Analysis of High-Power Bremsstrahlung Converters // *Problems of Atomic Science & Technology. Series «Nuclear Physics Investigations»*. 2008, №5 (50), p.155-159.
2. V.L. Uvarov. Installation for Isotope Production. Patent of Ukraine №20879, 2007.

3. M.I. Ayzatskiy, E.Z. Biller, V.N. Boriskin, et al. High-Power Electron S-band Linac for Industrial Purposes // *Proc. of the 2003 PAC*, Portland, Oregon, USA, May 12-16, 2003, p.2878-2880.
4. F. Salvat, J.M. Fernández-Varea and J. Sempau. *PENELOPE-2006 A Code System for Monte Carlo Simulation of Electron and Photon Transport*: OECD Nuclear Energy Agency, Issy-les-Moulineaux, France, 2006.
5. V.I. Nikiforov, V.L. Uvarov. Analysis of Mixed e, X-Radiation along the Extraction Facilities of Electron Accelerators // *Atomic Energy*. 2009, v.106, №4, p.220-224.
6. V.V. Kharitonov, Yu.V. Kiselyova, V.V. Atamanov, et al. A Generalization of Results of the Heat Exchange Intensification in the Channels with Porous Inserts // *Thermophysics of High Temperatures*. 1994, v.32, №3, p.433-440.
7. L.S. Kokorev, V.I. Subbotin, V.N. Fedoseyev, et al. On Interdependence of Hydraulic Resistance and Heat Emission in the Porous Mediums // *Thermophysics of High Temperatures*. 1994, v.25, №1, p.92-97.
8. V.I. Nikiforov, R.I. Pomatsalyuk, V.A. Shevchenko, et al. Measuring System of High-Energy Bremsstrahlung Profile // *Problems of Atomic Science & Technology. Series «Nuclear Physics Investigations»*. 2008, №3 (49), p.201-205.

*Статья поступила в редакцию 07.09.2009 г.*

### **РАСПРЕДЕЛЕННЫЙ КОНВЕРТЕР ДЛЯ ГЕНЕРАЦИИ ТОРМОЗНОГО ИЗЛУЧЕНИЯ С БОЛЬШОЙ ЯРКОСТЬЮ**

***Е.З. Биллер, В.И. Никифоров, А.Э. Тенишев, А.В. Торговкин, В.Л. Уваров, В.А.Шевченко, И.Н. Шляхов, Б.И. Шраменко, В.Ф. Жигло***

Разработан и исследован принципиально новый тип конвертера плотного пучка электронов в тормозное излучение. Для повышения тепловой стойкости конвертера путем увеличения эффективности теплообмена в области генерации излучения тормозящая среда выполнена в виде дроби, равномерно распределенной в охлаждающей воде. Приведены результаты компьютерного моделирования, теплофизического анализа и экспериментальных исследований варианта конвертера на основе свинцовой дроби. Показана возможность существенного увеличения допустимой плотности пучка электронов, а также снижения наведенной активности и расхода охлаждающей воды по сравнению с пластинчатым конвертером из тантала.

### **РОЗПОДІЛЕНИЙ КОНВЕРТЕР ДЛЯ ГЕНЕРАЦІЇ ГАЛЬМІВНОГО ВИПРОМІНЕННЯ З ВЕЛИКОЮ ЯСКРАВИСТЮ**

***Є.З. Біллер, В.І. Нікіфоров, А.Є. Тенішев, О.В. Торговкін, В.Л. Уваров, В.А.Шевченко, І.М. Шляхов, Б.І. Шраменко, В.Ф. Жигло***

Розроблено і досліджено принципово новий тип конвертера щільного пучка електронів у гальмівне випромінювання. Для підвищення теплової стійкості конвертера шляхом збільшення ефективності теплообміну в області генерації випромінювання гальмуюче середовище виконане у вигляді дроби, рівномірно розподіленого у воді, що охолоджує. Приведені результати комп'ютерного моделювання, теплофізичного аналізу і експериментальних досліджень варіанту конвертера на основі свинцевого дроби. Показана можливість істотного збільшення допустимої щільності пучка електронів, а також зниження наведеної активності і витрати води, що охолоджує, в порівнянні з пластинчастим конвертером з танталу.